ISSN 2709-4170 (Print)
ISSN 2791-0709 (online)
https://doi.org/10.52587/tmcs030102
Transactions in Mathematical and Computational Sciences
Vol. 03(1)(2024) pp. 16–39

MATHEMATICAL EXPLORATION OF TOPOLOGICAL INDICES IN TETRA-CYANO-BENZENE TRANSITION METAL ORGANIC NETWORKS

MOHAMMED ALI ALGHAMDI[1,*], DINA ABUZAID[1] ABDUL QADEER[2], MUHAMMAD FAISAL NADEEM[2]

[1] Department of Mathematics, Faculty of Science, King Abdulaziz University, Jeddah 21589, Saudi Arabia
mamalgamdi@kau.edu.sa, dabuzaid@kau.edu.sa
[2]Department of Mathematics, COMSATS University Islamabad, Lahore Campus, Lahore 54000 Pakistan
mfaisalnadeem@ymail.com

Abstract. Metal-Organic Frameworks have already shown enormous possibilities, starting from catalysis to drug delivery. This paper outlines the topological indices in the case of tetra-cyano-benzene transition metal organic networks due to the unique properties that they exhibit in electronic, magnetic, and catalytic applications. A detailed mathematical investigation of topological indices such as atom-bond connectivity, geometric arithmetic index, and others is presented in relation to tetra-cyano-benzene and its complexation with transition metals.
Keywords: Tetra-cyano-benzene, transition metal organic network, topological indices.

1. INTRODUCTION

Metal-Organic Frameworks (MOFs) are a class of porous materials [1] consisting of metal ions or clusters coordinated to organic ligands, or often called organic linkers [2]. These structures create highly ordered, three-dimensional frameworks with enormous internal surface areas and tunable pore sizes [3]. From gas storage [4] and separation to catalysis [5], drug delivery [6], and environmental remediation [7], their versatility and potential seem boundless. Their difference lies in their unique ability to be tailored at the

*Correspondence: mamalgamdi@kau.edu.sa
Received: 31.10.2024 Revised: 17.11.2024 Accepted: 25.11.2024 Published: 22.12.2024

molecular level, hence creating very specific control over properties related to their chemical stability and functionality. The potential of MOFs is presently under consideration for use in solving some of the major global challenges bound to energy storage [8], carbon capture [9], and development of sustainable materials.

The organic compound Tetra-cyano-benzene (TCNB) contains a benzene ring attached with four cyano groups at the 1,2,4,5-positions. Its complexation with transition metals will offer exciting coordination, chemistry and materials with unique properties. TCNB and its transition metal complexes have been interesting due to the opportunity to engage in various chemical processes and find an application in molecular electronics, catalysis, and magnetic materials. Interest in the study of tetra-cyano-benzene within the frame of coordination chemistry started in the middle of the 20th century when scientists conducted research on substances with cyano groups.

The transition metals are well-known for their variable oxidation states [10] and coordination capability; hence, in combination with TCNB, they have been used to explore their properties in coordination networks and supramolecular assemblies [11]. In fact, these products feature interesting electronic, magnetic, and optical properties-constituting a cogent reason for continued research into finding their applications. In TCNB-based transition metal complexes, there has been promise regarding application in molecular electronics due to their nature of efficiently transporting electrons. It is because such compounds can develop conductive frameworks and, possibly, may find applications in nanoscale electronic devices: as organic semiconductors or switches. Transition metal-TCNB complexes catalyze a wide range of chemical reactions, especially organic syntheses. More precisely, active intermediates are stabilized, and electron transfer processes promoted; therefore, they act in catalytic cycles, especially those that include redox reactions. This implies that the strong electronic interaction between TCNB and transition metals may give rise to interesting magnetic properties. Stimulated by the possible diversities of magnetic functionalities, for instance in spintronic devices and magnetic storage systems, several TCNB-metal complexes have been prepared so far with the purpose of material design [12]. TCNB and its transition metal complexes continue to be of high interest regarding designed advanced materials with tailored properties by virtue of meeting scientific and industrial needs.

Topological indices are invariants derived on the basis of a chemical graph; as a result, the structure of molecules is represented without reference to any geometric and spatial properties. These indices will give some very important information concerning connectivity and arrangement of atoms in a molecule and, as a consequence, certain properties and express the behavior of a molecule. Topological indices have become an integral part of cheminformatics [13] and QSAR studies, in which these indices predict the biological activity, toxicity, or physicochemical properties of chemical compounds without referring

to any experimental data. As examples, topological indices most often model drug efficacy [14], predict chemical reactivity, or assess risk to the environment related to specified molecules.

Moreover, topological indices find their application in materials science to predict properties of a new material. In view of the analysis on a molecular level, one is able to foresee its thermal stability, conduction, or strength. In nanotechnology, they enable the design of nanomaterials with desired properties by finding their best molecular arrangement. Topological indices have thus become one of the most powerful means to understand molecular behavior, enabling various shortcuts of research and rational design of chemicals and materials.

Indices like the atom-bond connectivity (ABC) and geometric arithmetic (GA) indices are often linked to thermodynamic stability and binding energies of molecules, aiding in the assessment of molecular reactivity and stability. Tools such as the forgotten topological index (F) and augmented Zagreb index (AZI) are employed in Quantitative Structure-Property Relationships (QSPR) and Quantitative Structure-Activity Relationships (QSAR) to model drug efficacy, toxicity, and other biological activities.

Topological and QSPR/QSAR analysis of antiviral drugs against COVID-19 treatment was conducted by Kirmani et al. [14]. New topological indices based on resistance distance suited for complete bipartite networks were proposed by Zaman, Raza and Ullah [15]. Meharban et al., [16] performed some new topological descriptors and regression models in the molecular structural modeling and physical characteristics analysis of some anti-breast cancer drugs. Ullah, Bano, and Zaman [17] studied the computational aspects of two major biochemical networks using some new molecular descriptors. Hayat et al. [18] illustrated the predictive aptitude of some distance-related spectral graphical descriptors in modeling thermodynamic properties of polycyclic hydrocarbons. Zaman et al. [19] studies neighborhood irregular topological indices in nanostructures TUC4C8 [p, q] and GTUC [p, q] mathematically and empirically. Pandi et al. [20] presented structure-property models for the pharmacokinetic properties of anticancer drugs using topological indices, multigraph modeling, and multi-criteria decision making. Two new temperature-based topological indices were put forward by Hayat, Alanazi, and Liu [21], which appeared powerful in prediction of the physicochemical properties of polycyclic aromatic hydrocarbons and their applications to silicon carbide nanotubes. Another one is the comparative analysis of temperature-based graphical indices to correlate total π electron energy of benzenoid hydrocarbons by Hayat and Liu [22]. Zaman et al. [23] presented new resistance distance-based topological indices for certain graph networks that enrich the knowledge about their structure. For more details see [24–29].

Definition 1. Estrada et al. in 1998, introduced the atom bond connectivity index and defined as;

$$ABC(\chi) = \sum_{uv \in E(\chi)} \sqrt{\frac{\lambda_u + \lambda_v - 2}{\lambda_u \times \lambda_v}}. \tag{1}$$

Definition 2. The geometric arithmetic index *GA* of a graph χ is introduced by Vukičević et al. [30] in 2009 and defined as below,

$$GA(\chi) = \sum_{uv \in E(\chi)} \frac{2\sqrt{\lambda_u \times \lambda_v}}{\lambda_u + \lambda_v}. \tag{2}$$

Definition 3. Furtula and Gutman [31], presented forgotten topological index in 2015, and formulated as;

$$F(\chi) = \sum_{uv \in E(\chi)} (\lambda_u^2 + \lambda_v^2). \tag{3}$$

Definition 4. Furtula [32] et al. defined augmented Zagreb index in 2010, and formulated as given below;

$$AZI(\chi) = \sum_{uv \in E(\chi)} \left(\frac{\lambda_u \times \lambda_v}{\lambda_u + \lambda_v - 2} \right)^3. \tag{4}$$

Definition 5. Balaban [33, 34], defined the Balaban index for a graph χ of order n_χ, size m_χ in 1982, and formulated as:

$$J(\chi) = \frac{m_\chi}{m_\chi - n_\chi + 2} \sum_{uv \in E(\chi)} \frac{1}{\sqrt{\lambda_u \times \lambda_v}}. \tag{5}$$

Definition 6. The symmetric division index *SDI* of a graph χ is introduced by Vukičević et al. [35] in 2010, and defined by the following way;

$$SDI(\chi) = \sum_{uv \in E(\chi)} \frac{\lambda_u^2 + \lambda_v^2}{\lambda_u \times \lambda_v}. \tag{6}$$

Definition 7. The sum-connectivity index was introduced by Zhou and Trinajstić [36], and described as;

$$SCI(\chi) = \sum_{uv \in E(\chi)} \frac{1}{\sqrt{\lambda_u \times \lambda_v}}. \tag{7}$$

Definition 8. The general sum-connectivity index $\chi_a(\chi)$ for a graph χ, was proposed in 2010 in [37], and defined in following manner;

$$\chi_a(\chi) = \sum_{uv \in E(\chi)} (\lambda_u + \lambda_v)^\alpha. \tag{8}$$

TABLE 1. Edge partition of $TCNB(\alpha,\beta)$

$(\lambda_u,\ \lambda_v)$	Frequency	Set of Edges
$(1,3)$	$2\alpha+2\beta+4\alpha\beta$	Xi_1
$(2,3)$	$8\alpha+8\beta+8\alpha\beta+8$	Xi_2
$(2,2)$	$4\alpha+4\beta+8$	XI_3
$(3,3)$	$14\alpha+14\beta+28\alpha\beta$	Xi_4
$(3,4)$	$4\alpha+4\beta+4\alpha\beta+4$	Xi_5

Definition 9. The first Gourava index of a graph χ defined in [38] and described in the following manner;

$$GO_1(\chi)=\sum_{uv\in E(\chi)}(\lambda_u+\lambda_v+\lambda_u\times\lambda_v). \tag{9}$$

Definition 10. The second Gourava index of a molecular graph χ is defined in [38] and presented as below;

$$GO_2(\chi)=\sum_{uv\in E(\chi)}(\lambda_u^2\times\lambda_v+\lambda_u\times\lambda_v^2). \tag{10}$$

Definition 11. The first and second hyper-Gourava indices of a molecular graph χ is defined in [39] as;

$$HGO_1(\chi)=\sum_{uv\in E(\chi)}[(\lambda_u+\lambda_v+\lambda_u\times\lambda_v]^2. \tag{11}$$

$$HGO_2(\chi)=\sum_{uv\in E(\chi)}[((\lambda_u+\lambda_v)\times\lambda_u\times\lambda_v]^2. \tag{12}$$

2. TRANSITION METAL - TETRA-CYANO-BENZENE (TM-TCNB)

Figure 1 and 2 illustrates the chemical structure for TM-TCNB and its graph representation, respectively. This structure horizontal extension with $m\geq 1$ and vertical extension with $n\geq 1$. TM-TCNB has $25\alpha+25\beta+32\alpha\beta+17$ vertices and $32\alpha+32\beta+44\alpha\beta+20$ edges. The vertices fall into the four degree types, from 1 to 4, that are listed in Table 2. Notably, a total of five different edge types may be identified based on the degrees of their two bounding vertices, and these are summarized in Table 1.
Now, we move towards the main results of different topological indices.

Theorem 2.1. *Let $TCNB(\alpha,\beta)$ be a tetra-cyano-benzene transition metal organic network for $\alpha,\beta\geq 1$. Then*

$$ABC(TCNB(\alpha,\beta))=30.7847\alpha+30.7847\beta+40.9225\alpha\beta+20.6469.$$

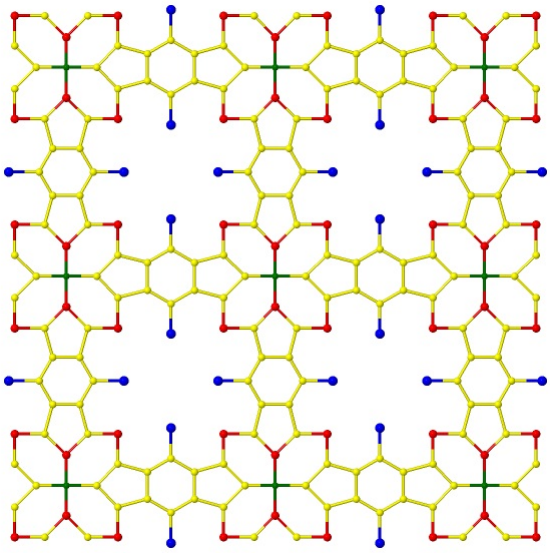

FIGURE 1. Transition metal - Tetra-cyano-benzene (TM-TCNB)

TABLE 2. Vertex partition of $TCNB(m,n)$

λ_u	Frequency	Set of Vertices
1	$2\alpha+2\beta+4\alpha\beta$	V_1
2	$8\alpha+8\beta+4\alpha\beta+12$	V_2
3	$14\alpha+14\beta+24\alpha\beta+4$	V_3
4	$\alpha+\beta+\alpha\beta+1$	V_4

Proof. Consider $TCNB(\alpha,\beta)$ be a tetra-cyano-benzene transition metal organic network for $\alpha,\beta \geq 1$. Using Tables 1 and 2 for degree type and edge type respectively, putting the

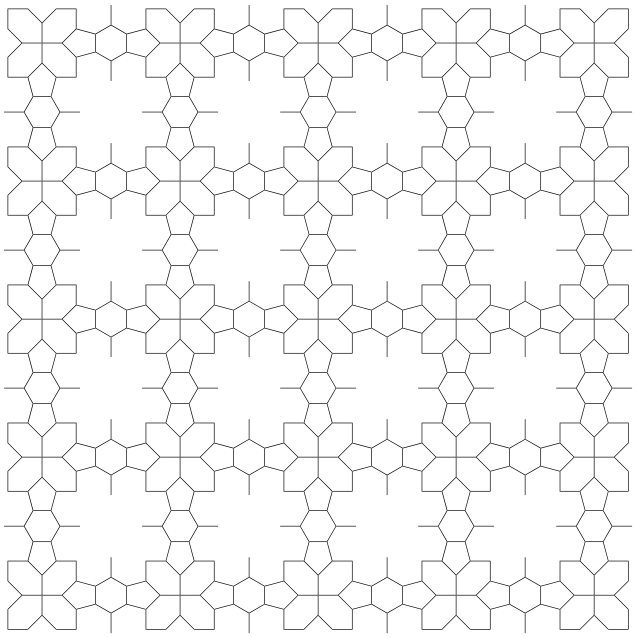

FIGURE 2. Graph of Transition metal - Tetra-cyano-benzene (TM-TCNB)

values in Equation (1). Then

$$\begin{aligned} ABC(TCNB(\alpha,\beta)) &= (2\alpha+2\beta+4\alpha\beta)\left(\sqrt{\frac{1+3-2}{1\times 3}}\right)+(8\alpha+8\beta+8\alpha\beta+8)\\ &\left(\sqrt{\frac{2+3-2}{2\times 3}}\right)+(4\alpha+4\beta+8)\left(\sqrt{\frac{2+2-2}{2\times 2}}\right)\\ &+(14\alpha+14\beta+28\alpha\beta)\left(\sqrt{\frac{3+3-2}{3\times 3}}\right)+(4\alpha+4\beta+4\alpha\beta+4)\\ &\left(\sqrt{\frac{3+4-2}{3\times 4}}\right),\\ &= 30.7847\alpha+30.7847\beta+40.9225\alpha\beta+20.6469. \end{aligned}$$

□

Theorem 2.2. *Let $TCNB(\alpha,\beta)$ be a tetra-cyano-benzene transition metal organic network for $\alpha,\beta \geq 1$. Then*

$$GA(TCNB(\alpha,\beta)) = 31.5292\alpha + 31.5292\beta + 43.2612\alpha\beta + 19.7972.$$

Proof. Consider tetra-cyano-benzene transition metal organic network ($TCNB(\alpha,\beta)$ for $\alpha,\beta \geq 1$ and degree type is given in Table 2 and edge type in Table 1. So from Equation (2)

$$\begin{aligned} GA(TCNB(\alpha,\beta)) &= (2\alpha+2\beta+4\alpha\beta)2\frac{\sqrt{1\times 3}}{1+3} + (8\alpha+8\beta+8\alpha\beta+8)2\frac{\sqrt{2\times 3}}{2+3} \\ &+ (4\alpha+4\beta+8)2\frac{\sqrt{2\times 2}}{2+2} + (14\alpha+14\beta+28\alpha\beta)2\frac{\sqrt{3\times 3}}{3+3} \\ &+ (4\alpha+4\beta+4\alpha\beta+4)2\frac{\sqrt{3\times 4}}{3+4}, \\ &= 31.5292\alpha + 31.5292\beta + 43.2612\alpha\beta + 19.7972. \end{aligned}$$

□

Theorem 2.3. *Let $TCNB(\alpha,\beta)$ be a tetra-cyano-benzene transition metal organic network for $\alpha,\beta \geq 1$. Then*

$$F(TCNB(\alpha,\beta)) = 508\alpha + 508\beta + 708\alpha\beta + 268.$$

Proof. Consider tetra-cyano-benzene transition metal organic network. Using Table 1 and Table 2 for degree type and edge type for the Equation (3). Then

$$\begin{aligned} F(TCNB(\alpha,\beta)) &= (2\alpha+2\beta+4\alpha\beta)(1^2+3^2) + (8\alpha+8\beta+8\alpha\beta+8)(2^2+3^2) \\ &+ (4\alpha+4\beta+8)(2^2+2^2) + (14\alpha+14\beta+28\alpha\beta)(3^2+3^2) \\ &+ (4\alpha+4\beta+4\alpha\beta+4)(3^2+4^2), \\ &= 508\alpha + 508\beta + 708\alpha\beta + 268. \end{aligned}$$

□

Theorem 2.4. *Let $TCNB(\alpha,\beta)$ be a tetra-cyano-benzene transition metal organic network for $\alpha,\beta \geq 1$. Then*

$$AZI(TCNB(\alpha,\beta)) = 143.2630\alpha + 143.2630\beta + 174.5130\alpha\beta + 112.0130.$$

Proof. Consider $TCNB(\alpha,\beta)$ be a tetra-cyano-benzene transition metal organic network with degree type in Table 2 and edge type in Table 1. Putting values in Equation (4). Then

$$\begin{aligned}AZI(TCNB(\alpha,\beta)) &= (2\alpha+2\beta+4\alpha\beta)\left(\frac{1+3}{1+3-2}\right)^3+(8\alpha+8\beta+8\alpha\beta+8)\\ &\left(\frac{2+3}{2+3-2}\right)^3+(4\alpha+4\beta+8)\left(\frac{2+2}{2+2-2}\right)^3+(14\alpha+14\beta+28\alpha\beta)\\ &\left(\frac{3+3}{3+3-2}\right)^3+(4\alpha+4\beta+4\alpha\beta+4)\left(\frac{3+4}{3+4-2}\right)^3,\\ &= 143.2630\alpha+143.2630\beta+174.5130\alpha\beta+112.0130.\end{aligned}$$

□

Theorem 2.5. *Let $TCNB(\alpha,\beta)$ be a tetra-cyano-benzene transition metal organic network for $\alpha,\beta\geq 1$. Then*

$$\begin{aligned}J(TCNB(\alpha,\beta)) &= \frac{(32\alpha+32\beta+44\alpha\beta+20)(\alpha+\beta+2\alpha\beta)}{11\alpha\beta+7\alpha+7\beta+3}\\ &+\frac{8\sqrt{5}(32\alpha+32\beta+44\alpha\beta+20)(\alpha+\beta+\alpha\beta+1)}{5(7\alpha+7\beta+11\alpha\beta+3)}+\\ &+\frac{2(32\alpha+32\beta+44\alpha\beta+20)(\alpha+\beta+2)}{7\alpha+7\beta+11\alpha\beta+3}\\ &+\frac{28\sqrt{6}(8\alpha+8\beta+11\alpha\beta+5)(\alpha+\beta+2\alpha\beta)}{3(7\alpha+7\beta+11\alpha\beta+3)}\\ &+\frac{4\sqrt{7}(32\alpha+32\beta+44\alpha\beta+20)(\alpha+\beta+\alpha\beta)}{7(7\alpha+7\beta+11\alpha\beta+3)}.\end{aligned}$$

Proof. Consider tetra-cyano-benzene transition metal organic network. The order of the graph $|V(TCNB(\alpha,\beta))|$ is $25\alpha+25\beta+33\alpha\beta+17$ and the size of the graph $E|(TCNB(\alpha,\beta))|$ is $32\alpha+32\beta+44\alpha\beta+20$. Then by equation (5)

$$\begin{aligned}&J(TCNB(\alpha,\beta)) = \left(\tfrac{32\alpha+32\beta+44\alpha\beta+20}{32\alpha+32\beta+44\alpha\beta+20-(25\alpha+25\beta+33\alpha\beta+17)}\right)\times(2\alpha+2\beta+4\alpha\beta)\\ &\left(\tfrac{1}{\sqrt{1+3}}\right)+\left(\tfrac{32\alpha+32\beta+44\alpha\beta+20}{32\alpha+32\beta+44\alpha\beta+20-(25\alpha+25\beta+33\alpha\beta+17)}\right)\times(8\alpha+8\beta+8\alpha\beta+1)\left(\tfrac{1}{\sqrt{2+3}}\right)\\ &+\left(\tfrac{32\alpha+32\beta+44\alpha\beta+20}{32\alpha+32\beta+44\alpha\beta+20-(25\alpha+25\beta+33\alpha\beta+17)}\right)\times(4\alpha+4\beta+8)\left(\tfrac{1}{\sqrt{2+2}}\right)\\ &+\left(\tfrac{32\alpha+32\beta+44\alpha\beta+20}{32\alpha+32\beta+44\alpha\beta+20-(25\alpha+25\beta+33\alpha\beta+17)}\right)\times(14\alpha+14\beta+28\alpha\beta)\left(\tfrac{1}{\sqrt{3+3}}\right)\\ &+\left(\tfrac{32\alpha+32\beta+44\alpha\beta+20}{32\alpha+32\beta+44\alpha\beta+20-(25\alpha+25\beta+33\alpha\beta+17)}\right)\times(4\alpha+4\beta+4\alpha\beta)\left(\tfrac{1}{\sqrt{3+4}}\right)\\ &=\tfrac{(32\alpha+32\beta+44\alpha\beta+20)(\alpha+\beta+2\alpha\beta)}{11\alpha\beta+7\alpha+7\beta+3}+\tfrac{8\sqrt{5}(32\alpha+32\beta+44\alpha\beta+20)(\alpha+\beta+\alpha\beta+1)}{5(7\alpha+7\beta+11\alpha\beta+3)}+\end{aligned}$$

$\frac{2(32\alpha+32\beta+44\alpha\beta+20)(\alpha+\beta+2)}{7\alpha+7\beta+11\alpha\beta+3}+\frac{28\sqrt{6}(8\alpha+8\beta+11\alpha\beta+5)(\alpha+\beta+2\alpha\beta)}{3(7\alpha+7\beta+11\alpha\beta+3)}+$
$\frac{4\sqrt{7}(32\alpha+32\beta+44\alpha\beta+20)(\alpha+\beta+\alpha\beta)}{7(7\alpha+7\beta+11\alpha\beta+3)}$. □

Theorem 2.6. *Let $TCNB(\alpha,\beta)$ be a tetra-cyano-benzene transition metal organic network for $\alpha,\beta \geq 1$. Then*

$$SDI(TCNB) = 90.0857\alpha + 90.0857\beta + 129.0857\alpha\beta + 51.0857.$$

Proof. Consider $TCNB(\alpha,\beta)$ be a tetra-cyano-benzene transition metal organic network for $\alpha,\beta \geq 1$ with degree type and edge type in Table 1 and Table 2 respectively. Then from Equation (6);

$$\begin{aligned} SDI(TCNB(\alpha,\beta)) &= (2\alpha+2\beta+4\alpha\beta)\frac{1^2+3^2}{1+3} + (8\alpha+8\beta+8\alpha\beta+8)\frac{2^2+3^2}{2+3} \\ &+ (4\alpha+4\beta+8)\frac{2^2+3^2}{2+2} + (14\alpha+14\beta+28\alpha\beta)\frac{3^2+3^2}{3+3} \\ &+ (4\alpha+4\beta+4\alpha\beta+4)\frac{3^2+4^2}{3+4}, \\ &= 90.0857\alpha + 90.0857\beta + 129.0857\alpha\beta + 51.0857. \end{aligned}$$

□

Theorem 2.7. *Let $TCNB(\alpha,\beta)$ be a tetra-cyano-benzene transition metal organic network for $\alpha,\beta \geq 1$. Then*

$$SCI(TCNB) = 13.8050\alpha + 13.8050\beta + 18.5205\alpha\beta + 9.0895.$$

Proof. Consider $TCNB(\alpha,\beta)$ be a tetra-cyano-benzene transition metal organic network for $\alpha,\beta \geq 1$. Its degree type and edge type are defined in Table 1 and Table 2 respectively. Then from Equation (7);

$$\begin{aligned} SCI(TCNB(\alpha,\beta)) &= (2\alpha+2\beta+4\alpha\beta)\frac{1}{\sqrt{1+3}} + (8\alpha+8\beta+8\alpha\beta+8)\frac{1}{\sqrt{2+3}} \\ &+ (4\alpha+4\beta+8)\frac{1}{\sqrt{2+2}} + (14\alpha+14\beta+28\alpha\beta)\frac{1}{\sqrt{3+3}} \\ &+ (4\alpha+4\beta+4\alpha\beta+4)\frac{1}{\sqrt{3+4}}, \\ &= 13.8050\alpha + 13.8050\beta + 18.5205\alpha\beta + 9.0895. \end{aligned}$$

□

Theorem 2.8. *Let $TCNB(\alpha,\beta)$ be a tetra-cyano-benzene transition metal organic network for $\alpha,\beta \geq 1$. Then*

$$X_\gamma(TCNB(\alpha,\beta)) = (6\alpha+6\beta+4\alpha\beta+8)(4)^\gamma + (8\alpha+8\beta+8\alpha\beta+8)(5)^\gamma + (14\alpha+14\beta+28\alpha\beta)(6)^\gamma + (4\alpha+4\beta+4\alpha\beta+4)(7)^\gamma.$$

Proof. Consider $TCNB(\alpha,\beta)$ be a tetra-cyano-benzene transition metal organic network for $\alpha,\beta \geq 1$ with degree type given in Table 2 and edge type in Table 1. Then by Equation (8);

$$\begin{aligned} X_\gamma(TCNB(\alpha,\beta)) &= (2\alpha+2\beta+4\alpha\beta)(1+3)^\gamma + (8\alpha+8\beta+8\alpha\beta+8)(2+3)^\gamma \\ &+ (4\alpha+4\beta+8)(2+2)^\gamma + (14\alpha+14\beta+28\alpha\beta)(3+3)^\gamma \\ &+ (4\alpha+4\beta+4\alpha\beta+4)(3+4)^\gamma, \\ &= (6\alpha+6\beta+4\alpha\beta+8)(4)^\gamma + (8\alpha+8\beta+8\alpha\beta+8)(5)^\gamma \\ &+ (14\alpha+14\beta+28\alpha\beta)(6)^\gamma + (4\alpha+4\beta+4\alpha\beta+4)(7)^\gamma. \end{aligned}$$

□

Theorem 2.9. *Let $TCNB(\alpha,\beta)$ be a tetra-cyano-benzene transition metal organic network for $\alpha,\beta \geq 1$. Then*

$$GO_1(TCNB(\alpha,\beta)) = 420\alpha+420\beta+612\alpha\beta+228.$$

Proof. Consider $TCNB(\alpha,\beta)$ be a Tetracynobenzene metallic organic compound for $\alpha,\beta \geq 1$ with degree type in Table 2 and edge type defined in Table 1. Then from Equation (9);

$$\begin{aligned} GO_1(TCNB(\alpha,\beta)) &= (2\alpha+2\beta+4\alpha\beta)(1+3+1\times 3) + (8\alpha+8\beta+8\alpha\beta+8) \\ &(2+3+2\times 3) + (4\alpha+4\beta+8)(2+2+2\times 2) + (14\alpha+14\beta+28\alpha\beta) \\ &(3+3+3\times 3)(4\alpha+4\beta+4\alpha\beta+4)(3+4+3\times 4), \\ &= 420\alpha+420\beta+612\alpha\beta+228. \end{aligned}$$

□

Theorem 2.10. *Let $TCNB(\alpha,\beta)$ be a tetra-cyano-benzene transition metal organic network for $\alpha,\beta \geq 1$. Then*

$$GO_2(TCNB(\alpha,\beta)) = 1420\alpha+1420\beta+2136\alpha\beta+704.$$

Proof. Consider $TCNB(\alpha,\beta)$ be a tetra-cyano-benzene transition metal organic network for $\alpha,\beta \geq 1$. Degree types are given in Table 2 and edge types defined in Table 1. Putting

the values in Equation (10), then

$$\begin{aligned} GO_2(TCNB(\alpha,\beta)) &= (2\alpha+2\beta+4\alpha\beta)(1^2\times 3+1\times 3^2)+(8\alpha+8\beta+8\alpha\beta+8)\\ &\quad (2^2\times 3+2\times 3^2)+(4\alpha+4\beta+8)(2^2\times 2+2\times 2^2)+\\ &\quad (14\alpha+14\beta+28\alpha\beta)(3^2\times 3+3\times 3^2)\\ &\quad (4\alpha+4\beta+4\alpha\beta+4)(3^2\times 4+3\times 4^2),\\ &= 1420\alpha+1420\beta+2136\alpha\beta+704. \end{aligned}$$

□

Theorem 2.11. *Let $TCNB(\alpha,\beta)$ be a tetra-cyano-benzene transition metal organic network for $\alpha,\beta\geq 1$. Then*

$$HGO_1(TCNB(\alpha,\beta)) = 5916\alpha+5916\beta+8908\alpha\beta+2924.$$

Proof. Consider tetra-cyano-benzene transition metal organic network ($TCNB(\alpha,\beta)$) for $\alpha,\beta\geq 1$ with degree type defined in Table 2 and edge type defined in Table 1. So from Equation (11);

$$\begin{aligned} HGO_1(TCNB(\alpha,\beta)) &= (2\alpha+2\beta+4\alpha\beta)[1+3+1\times 3]^2+(8\alpha+8\beta+8\alpha\beta+8)\\ &\quad [2+3+2\times 3]^2+(4\alpha+4\beta+8)[2+2+2\times 2]^2+\\ &\quad (14\alpha+14\beta+28\alpha\beta)[3+3+3\times 3]^2(4\alpha+4\beta+4\alpha\beta+4)\\ &\quad [3+4+3\times 4]^2,\\ &= 5916\alpha+5916\beta+8908\alpha\beta+2924. \end{aligned}$$

□

Theorem 2.12. *Let $TCNB(\alpha,\beta)$ be a tetra-cyano-benzene transition metal organic network for $\alpha,\beta\geq 1$. Then*

$$HGO_2(TCNB(\alpha,\beta)) = 77560\alpha+77560\beta+117648\alpha\beta+37472.$$

Proof. Consider tetra-cyano-benzene transition metal organic network ($TCNB(\alpha,\beta)$) for $\alpha,\beta\geq 1$ with degree type values in Table 2 and edge type values in Table 1. So from Equation (11);

$$\begin{aligned} HGO_2(TCNB(\alpha,\beta)) &= (2\alpha+2\beta+4\alpha\beta)[1+3\times 1\times 3]^2+(8\alpha+8\beta+8\alpha\beta+8)\\ &\quad [2+3\times 2\times 3]^2+(4\alpha+4\beta+8)[2+2\times 2\times 2]^2+(14\alpha+\\ &\quad 14\beta+28\alpha\beta)[3+3\times 3\times 3]^2(4\alpha+4\beta+4\alpha\beta+4)[3+4\times 3\times 4]^2,\\ &= 77560\alpha+77560\beta+117648\alpha\beta+37472. \end{aligned}$$

□

TABLE 3. Comparison of atom-bond connectivity and geometric arithmetic indices

(α,β)	$ABC(TCNB(\alpha,\beta))$	$GA(TCNB(m,n))$
$(1,1)$	123.14	126.12
$(1,2)$	194.85	200.91
$(2,2)$	307.48	318.96
$(2,3)$	420.11	437.01
$(3,3)$	573.66	598.32
$(3,4)$	727.21	759.64
$(4,4)$	921.68	964.21
$(4,5)$	1116.2	1168.8
$(5,5)$	1351.6	1416.6
$(5,6)$	1587.0	1664.5

Table 3 calculated values of two very important topological indices, ABC and GA indices, for the TCNB transition metal organic network. Values are shown for varying parameters α and β, which control the size of the molecular network. These indices bear critical information about molecular stability and reactivity. In most cases, the ABC index has been related to the thermodynamic stability of a molecule, while the GA index can be employed for the prediction of molecular properties such as binding energies. Both the ABC and GA indices are increasing with the rise in α and β values, regarding the growing complexity and potential functional capability of the molecular framework.

Fig. 3 plot of data presented in Table 3. Variation of ABC and GA indices with increase in molecular structure for larger values of α and β. Graphical trends clearly displayed that Geometric Arithmetic index has always higher values as compared to the Atom-Bond Connectivity index, which reflects the fact that GA index is more sensitive towards changes in molecular complexity.

Table 4 shows the Balaban index versus Symmetric Division Index (SDI) for different parameter values and associated to TCNB transition metal networks. While the Balaban index is a highly discriminative distance-based topological index, SDI describes the molecular connectivity with emphasis on the sum of vertex degrees. The larger the values of α and β are, the higher the values of both J and SDI; however, the values of SDI are appreciably higher than J due to a more detailed description of molecular symmetry and connectivity by SDI.

Figure 4 contrasts the trends of the Balaban and the Symmetric Division indices, as represented in Table 4. The rapid growth of in SDI testifies for this index sensitivity towards large connected molecular frameworks. In turn, the increase of the Balaban index is smoother - thus the latter index is appropriate for depicting the essential topological features of the molecular structure.

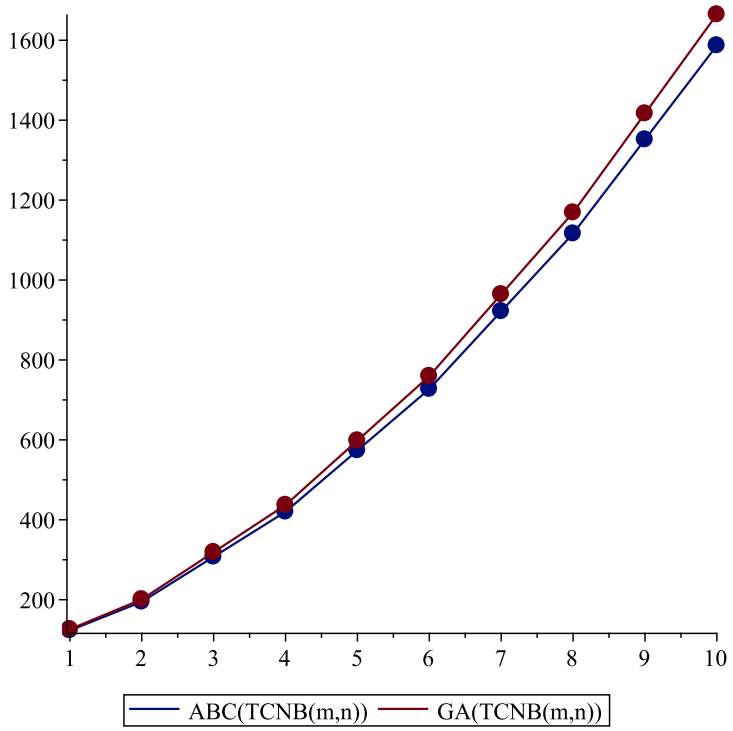

FIGURE 3. Graphical comparison of the Atom-Bond Connectivity (ABC) and Geometric Arithmetic (GA) indices

TABLE 4. Comparison of Balaban and symmetric division indices

(α,β)	$J(TCNB(\alpha,\beta))$	$SDI(TCNB(\alpha,\beta))$
$(1,1)$	245.52	360.34
$(1,2)$	381.54	579.51
$(2,2)$	591.32	927.77
$(2,3)$	801.46	1276.0
$(3,3)$	1085.5	1753.4
$(3,4)$	1369.7	2230.7
$(4,4)$	1727.9	2837.1
$(4,5)$	2086.1	3443.6
$(5,5)$	2518.5	4179.1
$(5,6)$	2950.9	4914.6

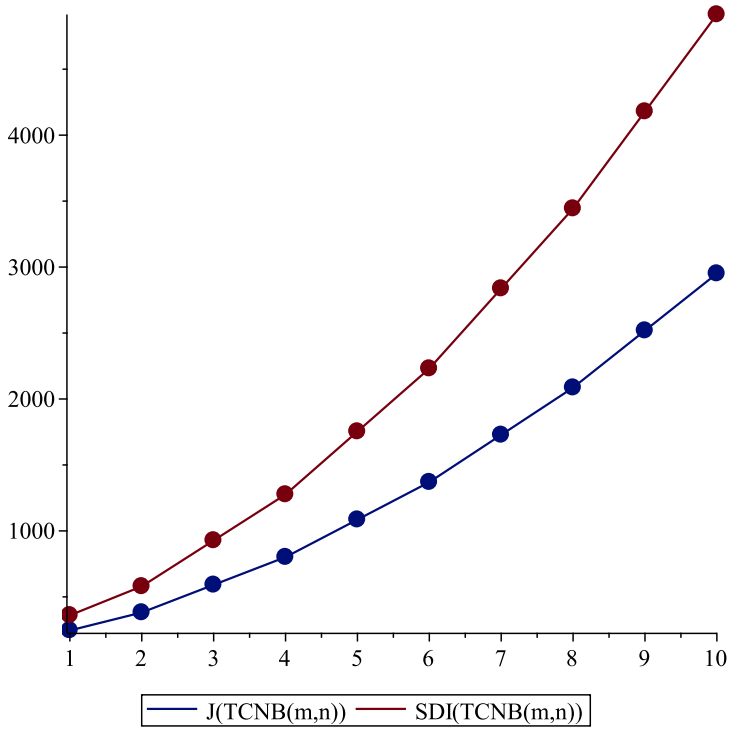

FIGURE 4. Graphical comparison of Balaban and symmetric division indices

Table 5 compares the first and second Gourava indices, both topological indices which account for the contribution of vertex degree as well as edge connections. The Gourava indices are very important to model various molecular properties such as reactivity and stability. Similar to all the other indices herein discussed, both GO1 and GO2 increase with larger α and β, but GO2 shows a significantly greater increase because of its dependence on the quadratic form of vertex degrees.

Figure 5 gives graphically the data from Table 5. One can notice in this figure that both GO1 and GO2 indices strongly increase with the increase in size of the molecular structure. The high value of GO2 compared to GO1 again underlines a greater sensitivity of the second Gourava index to the complexity of the molecular structure. Table 6 reports the first, HGO1, and the second Hyper-Gourava indices, HGO2, by far advanced topological descriptors based on the classical Gourava indices but with extended capabilities toward higher-degree interactions among vertices and edges. Such an index is of particular use

TABLE 5. Comparison of Gourava first and second indices

(α,β)	$GO_1(TCNB(\alpha,\beta))$	$GO_2(TCNB(\alpha,\beta))$
$(1,1)$	1680.0	5680.0
$(1,2)$	2712.0	9236.0
$(2,2)$	4356.0	14928.0
$(2,3)$	6000.0	20620.0
$(3,3)$	8256.0	28448.0
$(3,4)$	10512.0	36276.0
$(4,4)$	13380.0	46240.0
$(4,5)$	16248.0	56204.0
$(5,5)$	19728.0	68304.0
$(5,6)$	23208.0	80404.0

TABLE 6. Comparison of hyper Gourava first and second indices

(α,β)	$HGO_1(TCNB(\alpha,\beta))$	$HGO_2(TCNB(\alpha,\beta))$
$(1,1)$	23664.0	310240.0
$(1,2)$	38488.0	505450.0
$(2,2)$	62220.0	818300.0
$(2,3)$	85952.0	1131200.0
$(3,3)$	118590.0	1561700.0
$(3,4)$	151230.0	1992200.0
$(4,4)$	192780.0	2540300.0
$(4,5)$	234330.0	3088500.0
$(5,5)$	284780.0	3754300.0
$(5,6)$	335240.0	4420100.0

while modeling large and complex networks like TCNB-based frameworks. It follows from the data that both the HGO1 and HGO2 are considerably increased with α and β, but the increase of HGO2 with latter is sharper because of the inclusion of higher-order terms. Figure 6 depicts graphically the trends developed by HGO1 and HGO2 from Table 6. Similar to what happened in case of Gourava indices discussed earlier, HGO2 shows a sharper increase in comparison to HGO1. This demonstrates that HGO2 is more sensitive towards the increase in size- complexity of the molecular network. This figure actually underlines the usability of Hyper-Gourava indices in large molecular frameworks analyses.

Table 7 compares the F with AZI with respect to the variation of the parameters α and β which control the extent of the network. The Forgotten index is basically a degree-based topological index that describes the impact of vertex degree on the gross molecular

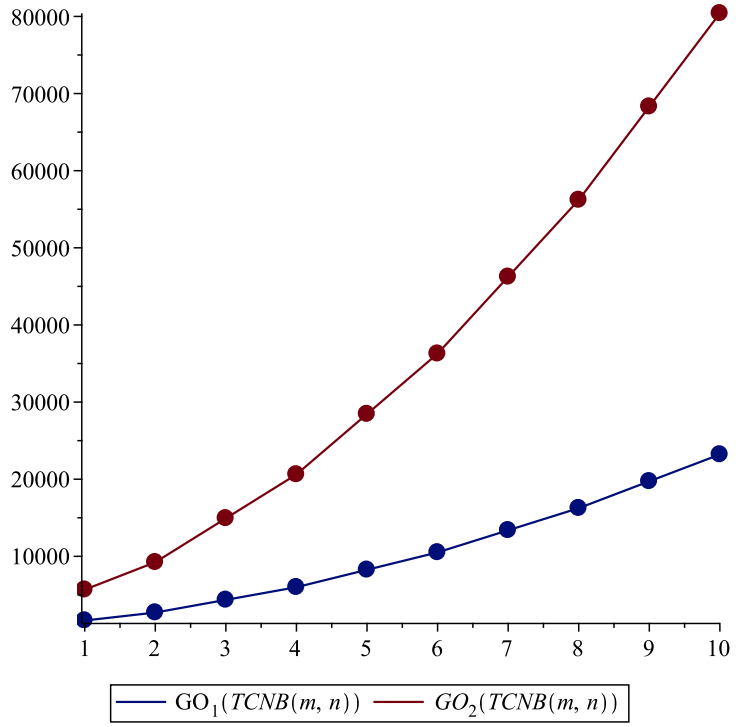

FIGURE 5. Graphical comparison of Gourava indices

architecture. It is of utmost utility in the analysis related to the stability regarding the molecule and bond-order distribution. On the other hand, it gives ideas on the sum of the degree of neighboring vertices useful in bonding connectivity and interaction in the molecule. As As functions of both α and βincrease, both indices increase; however, the Forgotten index does so in a much sharper fashion, reflecting its higher sensitivity to the variations at least in molecular size and complexity. Figure 7 gives the growth of the forgotten index along with that of AZI with an increasing size of molecular network. It is observed from this figure that the nature of growth for the index under consideration is much steeper than that of AZI. This clearly shows the high degree of sensitivity the index has for the minute details in molecular connectivities. Comparison in graphical ways reflects that the forgotten index grows more rapidly when α and β are larger, thus more suitable for the analysis of big molecular systems. Table 8 compares two variants of generalized sum connectivity indices $\chi^{-1/2}$ and $\chi^{1/2}$ for different cases of α and β,

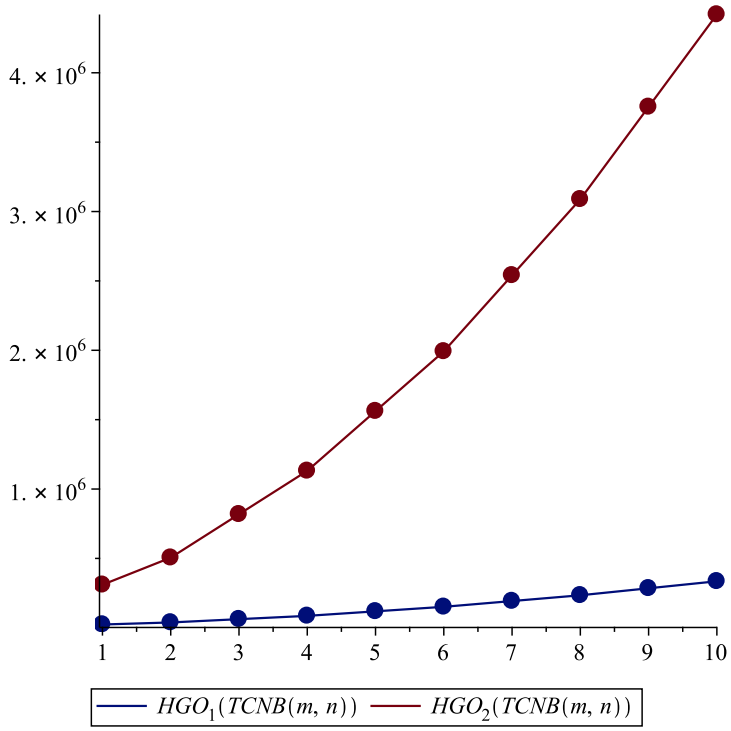

FIGURE 6. Graphical comparison of Hyper Gourava indices

TABLE 7. Comparison of Forgotten and augmented Zagreb indices

(α,β)	$F(TCNB(\alpha,\beta))$	$AZI(TCNB(\alpha,\beta))$
$(1,1)$	1992.0	573.05
$(1,2)$	3208.0	890.83
$(2,2)$	5132.0	1383.1
$(2,3)$	7056.0	1875.4
$(3,3)$	9688.0	2542.2
$(3,4)$	12320.0	3209.0
$(4,4)$	15660.0	4050.3
$(4,5)$	19000.0	4891.6
$(5,5)$	23048.0	5907.5
$(5,6)$	27096.0	6923.3

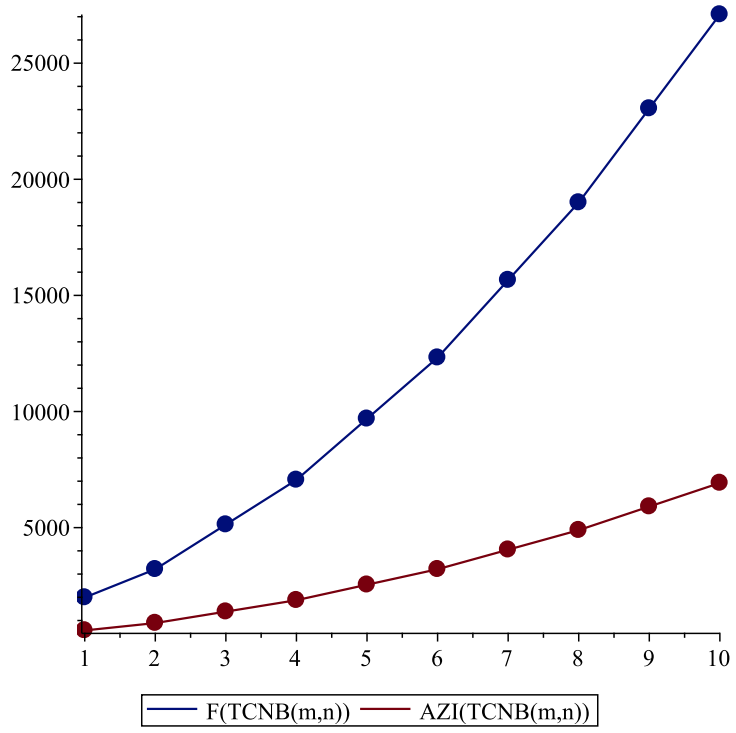

FIGURE 7. Graphical comparison of Forgotten and augmented Zagreb indices

and their use in studying the overall connectivity of a molecular network in respect to the distribution of vertex degree across the network. It follows that the contribution given by $\chi^{-1/2}$ is often smaller, while $\chi^{1/2}$ gives a bigger value of the contribution. Because of this, from the Table 8, $\chi^{1/2}$ can be seen to increase much more steeply than $\chi^{-1/2}$ with the increase in size; that is, from the view of molecular network, the effect imposed by the larger-degree vertices is much more crucial. Figure 8 also represents graphically the trends in the $\chi^{-1/2}$ and $\chi^{1/2}$ indices displayed in Table 8. One can observe from that figure that the $\chi^{1/2}$ index increases much stronger compared to $\chi^{-1/2}$, meaning that the last is more conservative while monitoring the changes of molecular size. Further, Fig.8 gives emphasis on the increasing role of higher-degree vertices for description of the overall connectivity of the TCNB transition metal network with growing complexity of the latter.

TABLE 8. Comparison of generalized sum connectivity indices for different α

(α,β)	$\chi_{-\frac{1}{2}}(TCNB(\alpha,\beta))$	$\chi_{\frac{1}{2}}(TCNB(\alpha,\beta))$
$(1,1)$	0.76454	22.039
$(1,2)$	0.62098	27.557
$(2,2)$	0.50601	34.375
$(2,3)$	0.43823	40.027
$(3,3)$	0.37974	46.588
$(3,4)$	0.33987	52.325
$(4,4)$	0.30425	58.760
$(4,5)$	0.27793	64.554
$(5,5)$	0.25391	70.915
$(5,6)$	0.23522	76.747

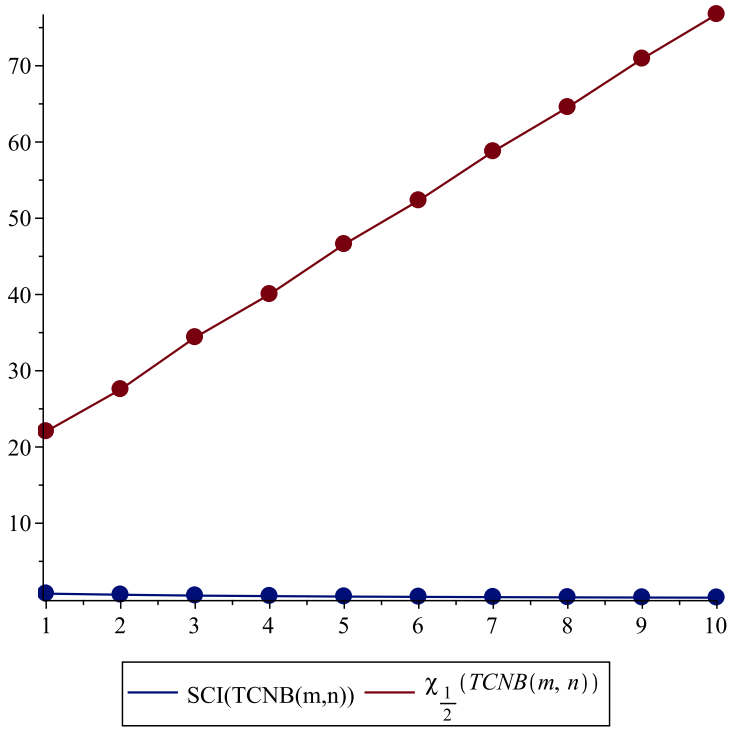

FIGURE 8. Graphical comparison of General sum-connectivity indices

3. Conclusion

The present work has rigorously reviewed the topological indices of tetracyano-benzene transition-metal organic networks. These findings may be applied to material design, characterization, and application. Further work might aim to investigate the predictive ability of the indices for newly emerging applications related to nanotechnology and catalysis. Advanced descriptors, such as hyper-Gourava indices, can also be employed in the design of efficient catalytic frameworks in either energy storage or environmental remediation. Further exploitation of those indices in the rational design of molecular electronics should allow the development of nanoscale devices with unprecedented conductivity and magnetic properties. Their mathematical modeling will also advance and provide ways to disclose new materials suitable for an encompassing variety of challenges from industry to science. We have calculated a number of topological indices and analyzed them in tetracyano-benzene transition metal organic networks. Included are the atom-bond connectivity index, geometric arithmetic index, and many others that give enough insight into molecular behavior with great application potential. These results demonstrate the usefulness of topological indices in predicting the stability, conductivity, and magnetic characteristics of these materials. The use of such elaborate mathematical modeling in this work adds not only to an understanding of these materials but also to their potential roles in the development of advanced technologies such as molecular electronics and nanotechnology. Further study in this way of such indices will allow further advance in the rational design of high-performance materials.

References

[1] Rowsell, J. L., & Yaghi, O. M. (2004). Metalorganic frameworks: a new class of porous materials. *Microporous and mesoporous materials,* ***73****(1-2)*, 3-14.

[2] Kitagawa, S. (2014). Metalorganic frameworks (MOFs). *Chemical Society Reviews,* ***43****(16),* 5415-5418.

[3] Alezi, D., Oppenheim, J. J., Sarver, P. J., Iliescu, A., Dinakar, B., & Dinca, M. (2023). Tunable lowrelative humidity and highcapacity water adsorption in a bibenzotriazole metalorganic framework. *Journal of the American Chemical Society,* ***145****(46),* 25233-25241.

[4] Felix Sahayaraj, A., Joy Prabu, H., Maniraj, J., Kannan, M., Bharathi, M., Diwahar, P., & Salamon, J. (2023). Metalorganic frameworks (MOFs): the next generation of materials for catalysis, gas storage, and separation. *Journal of Inorganic and Organometallic Polymers and Materials,* ***33****(7),* 1757-1781.

[5] Cheng, S., Ouyang, J., Li, M., Diao, Y., Yao, J., Li, F., ... & Quan, Y. (2023). Charge Separation in MetalOrganic Framework Enables Heterogeneous Thiol Catalysis. *Angewandte Chemie International Edition,* ***62****(25)*, e202300993.

[6] Vikal, A., Maurya, R., Patel, P., Paliwal, S. R., Narang, R. K., Gupta, G. D., & Kurmi, B. D. (2024). Exploring metal-organic frameworks (MOFs) in drug delivery: A concise overview of synthesis approaches, versatile applications, and current challenges. *Applied Materials Today*, **41**, 102443.

[7] Lal, S., Singh, P., Singhal, A., Kumar, S., Gahlot, A. P. S., Gandhi, N., & Kumari, P. (2024). Advances in metalorganic frameworks for water remediation applications. *RSC advances, **14**(5),* 3413-3446.

[8] Lu, Z. (2024). Experimental and theoretical analysis of Metal-Organic Frameworks energy storage performance for heating, cooling, power generation, and desalination. *Applied Thermal Engineering*, **240**, 122271.

[9] Tao, Y. R., & Xu, H. J. (2024). A critical review on potential applications of Metal-Organic frameworks (MOFs) in adsorptive carbon capture technologies. *Applied Thermal Engineering*, **236**, 121504.

[10] Riedel, S., & Kaupp, M. (2009). The highest oxidation states of the transition metal elements. *Coordination Chemistry Reviews, **253**(5-6)*, 606-624.

[11] Leininger, S., Olenyuk, B., & Stang, P. J. (2000). Self-assembly of discrete cyclic nanostructures mediated by transition metals. *Chemical Reviews, **100**(3)*, 853-908.

[12] Hoskins, B. F., & Robson, R. (1990). Design and construction of a new class of scaffolding-like materials comprising infinite polymeric frameworks of 3D-linked molecular rods. A reappraisal of the zinc cyanide and cadmium cyanide structures and the synthesis and structure of the diamond-related frameworks [N (CH3) 4][CuIZnII (CN) 4] and CuI [4, 4', 4", 4"'-tetracyanotetraphenylmethane] BF4. xC6H5NO2. *Journal of the American Chemical Society, **112**(4)*, 1546-1554.

[13] Estrada, E., & Uriarte, E. (2001). Recent advances on the role of topological indices in drug discovery research. *Current Medicinal Chemistry, **8**(13)*, 1573-1588.

[14] Kirmani, S. A. K., Ali, P., & Azam, F. (2021). Topological indices and QSPR/QSAR analysis of some antiviral drugs being investigated for the treatment of COVID19 patients. *International Journal of Quantum Chemistry, **121**(9)*, e26594.

[15] Zaman, S., Raza, A., & Ullah, A. (2024). Some new version of resistance distance-based topological indices of complete bipartite networks. *The European Physical Journal Plus, **139**(4)*, 357.

[16] Meharban, S., Ullah, A., Zaman, S., Hamraz, A., & Razaq, A. (2024). Molecular structural modeling and physical characteristics of anti-breast cancer drugs via some novel topological descriptors and regression models. *Current Research in Structural Biology*, **7**, 100134.

[17] Ullah, A., Bano, Z., & Zaman, S. (2024). Computational aspects of two important biochemical networks with respect to some novel molecular descriptors. *Journal of Biomolecular Structure and Dynamics*, **42**(2), 791-805.

[18] Hayat, S., Alanazi, S. J., Imran, M., & Azeem, M. (2024). Predictive potential of distance-related spectral graphical descriptors for structure-property modeling of thermodynamic properties of polycyclic hydrocarbons with applications. *Scientific Reports*, **14**(1), 22512.

[19] Zaman, S., Ullah, A., Naseer, R., & Rasool, K. B. (2024). Mathematical concepts and empirical study of neighborhood irregular topological indices of nanostructures TUC4C8 [p, q] and GTUC [p, q]. *Journal of Mathematics*, **2024**(1), 7521699.

[20] Pandi, U. P., Hayat, S., Marimuthu, S., & Konsalraj, J. (2024). Structureproperty modeling of pharmacokinetic characteristics of anticancer drugs via topological indices, multigraph modeling and multicriteria decision making. *International Journal of Quantum Chemistry*, **124**(11), e27428.

[21] Hayat, S., Alanazi, S. J., & Liu, J. B. (2024). Two novel temperature-based topological indices with strong potential to predict physicochemical properties of polycyclic aromatic hydrocarbons with applications to silicon carbide nanotubes. *Physica Scripta*, **99**(5), 055027.

[22] Hayat, S., & Liu, J. B. (2024). Comparative analysis of temperature-based graphical indices for correlating the total π-electron energy of benzenoid hydrocarbons. *International Journal of Modern Physics B*, 2550047.

[23] Zaman, S., Kamboh, A., Ullah, A., & Liu, J. B. (2023). Development of some novel resistance distance based topological indices for certain special types of graph networks. *Physica Scripta*, **98**(12), 125250.

[24] Liu, J. B., Yuan, X. Y., & Lee, C. C. (2024). Prediction of carbon emissions in China's construction industry using an improved grey prediction model. *Science of The Total Environment*, **938**, 173351.

[25] Rani, A., Imran, M., Razzaque, A., & Ali, U. (2021). Properties of Total Transformation Graphs for General Sum Connectivity Index. *Complexity*, **2021**(1), 6616056.

[26] Liu, J. B., Wang, X., & Cao, J. (2024). The Coherence and Properties Analysis of Balanced 2 p-Ary Tree Networks. IEEE *Transactions on Network Science and Engineering*, **11**(5) 4719-4728.

[27] Abbas, G., Rani, A., Salman, M., Noreen, T.,& Ali, U. (2021). Hosoya properties of the commuting graph associated with the group of symmetries. *Main Group Metal Chemistry*, **44**(1), 173-184.

[28] Liu, J. B., Zhang, X., & Cao, J. (2024). Structural properties of extended pseudofractal scale-free network with higher network efficiency. *Journal of Complex Networks*, **12**(3), cnae023.

[29] Ali, U., Baig, A. Q., Imran, M., Abbas, G., & Asif, M. (2017). On topological properties of certain boron nanostructures. *Journal of Computational and Theoretical Nanoscience*, **14**(2), 887-898.

[30] Vukievi, D., & Furtula, B. (2009). Topological index based on the ratios of geometrical and arithmetical means of end-vertex degrees of edges. *Journal of mathematical*

chemistry, **46**, 1369-1376.

[31] Furtula, B., & Gutman, I. (2015). A forgotten topological index. *Journal of mathematical chemistry*, **53**(4), 1184-1190.

[32] Furtula, B., Graovac, A., & Vukievi, D. (2010). Augmented zagreb index. *Journal of mathematical chemistry*, **48**, 370-380.

[33] Balaban, A. T., & Quintas, L. V. (1983). The smallest graphs, trees, and 4-trees with degenerate topological index. *Journal of Mathematical Chemistry*, **14**, 213-233.

[34] Balaban, A. T. (1982). Highly discriminating distance-based topological index. *Chemical physics letters*, **89**(5), 399-404.

[35] Vukicevic, D., & Gasperov, M. (2010). Bond additive modeling 1. Adriatic indices. *Croatica chemica acta*, **83**(3), 243.

[36] Zhou, B., & Trinajsti, N. (2009). On a novel connectivity index. *Journal of mathematical chemistry*, **46**, 1252-1270.

[37] Zhou, B., & Trinajsti, N. (2010). On general sum-connectivity index. *Journal of mathematical chemistry*, **47**, 210-218.

[38] Kulli, V. R. (2018). Reverse Zagreb and reverse hyper-Zagreb indices and their polynomials of rhombus silicate networks. *Annals of Pure and Applied Mathematics*, **16**(1), 47-51.

[39] Kulli, V. R., & On, K. (2016). On K hyper-Banhatti indices and coindices of graphs. *International Research Journal of Pure Algebra*, **6**(5), 300-304.